Bergische Universität Wuppertal

Fachbereich Mathematik und Naturwissenschaften

Lehrstuhl für Angewandte Mathematik
und Numerische Mathematik

Preprint BUW-AMNA 05/01

Roland Pulch

Variational Methods for Solving Warped Multirate PDAEs

April 2005

http://www.math.uni-wuppertal.de/org/Num/

Variational Methods for Solving Warped Multirate PDAEs

R. Pulch

Bergische Universität Wuppertal, Fachbereich Mathematik und Naturwissenschaften, Lehrstuhl für Angewandte Mathematik und Numerische Mathematik, Gaußstr. 20, D-42119 Wuppertal, Germany.

Abstract

Signals exhibiting amplitude as well as frequency modulation at widely separated time scales arise in radio frequency (RF) applications. A multivariate model yields an adequate representation by decoupling the time scales of involved signals. Consequently, a system of differential algebraic equations (DAEs) modelling the electric circuit changes into a system of partial differential algebraic equations (PDAEs). The determination of an emerging local frequency function is crucial for the efficiency of this approach, since inappropriate choices produce many oscillations in the multivariate solution. Thus the idea is to reduce oscillating behaviour via minimising the magnitude of partial derivatives. For this purpose, we apply variational calculus to obtain a necessary condition for a specific solution, which represents a minimum of an according functional. This condition can be included in numerical schemes computing the complete solution of the PDAE. Test results confirm that the used strategy ensures an efficient simulation of RF signals.

1 Introduction

Mathematical modelling of electric circuits is based on a network approach, which yields systems of differential algebraic equations (DAEs), see [2]. Thereby, the system describes the transient behaviour of all node voltages and some branch currents. In radio frequency (RF) applications, the amplitude and/or frequency of carrier waves is often modulated by slowly varying signals. Corresponding time scales differ by several orders of magnitude. Hence transient analysis of the

DAE system becomes inefficient, since high frequency oscillations limit the size of time steps, whereas the slow time scale determines the total time interval of the simulation.

A multivariate signal model permits an alternative approach by assigning an own variable to each separate time scale. Therefore the DAE system changes into a system of partial differential algebraic equations (PDAEs). Narayan and Roychowdhury [6] introduced the according warped multirate PDAE, where a local frequency function arises in addition to the multivariate signal representation. Corresponding multiperiodic solutions yield the desired RF signals of the DAE model via a reconstruction scheme. Since the time scales are decoupled in the multivariate approach, we can solve the PDAE system efficiently.

However, the efficiency of the PDAE model depends essentially on the determination of an adequate local frequency function. Unfavourable choices cause many oscillations in the corresponding multivariate signal representation. In contrast, a simple structure of the PDAE solution is required in order to use discretisations with relatively large step sizes. Continuous phase conditions, which are imposed on the multivariate representation, are applied efficiently to fix the local frequency function, cf. [6]. Numerical simulations verify that the resulting multivariate functions exhibit a simple form. Yet there is no guarantee for this advantageous quality of continuous phase conditions.

Alternatively, Houben [4] proposes a minimisation procedure, which reduces oscillatory behaviour in the multivariate functions. Thereby, the magnitude of according partial derivatives is minimised. This strategy is constructed for the solution of the PDAE including a mixture of initial and boundary conditions. On the other hand, we consider the direct computation of multiperiodic solutions, i.e. pure boundary value problems, in this paper.

Consequently, we identify the local frequency function using a similar minimum requirement with respect to partial derivatives of the corresponding multivariate signal representation. The employed construction is tailored to the determination of multiperiodic functions. An according functional is defined, which quantifies the magnitude of partial derivatives in the whole domain of dependence regarding the periodicities. The possible PDAE solutions are interconnected via a transformation formula. All solutions generate the same DAE solution in the reconstruction scheme. Based on the transformation, we apply variational calculus to develop a necessary condition for an optimal solution. This condition can be used in a numerical technique, which computes the multivariate signal representation as well as its corresponding local frequency function.

The paper is organised as follows. In Sect. 2, we illustrate the multivariate signal model briefly. Sect. 3 describes the PDAE model and its transformation

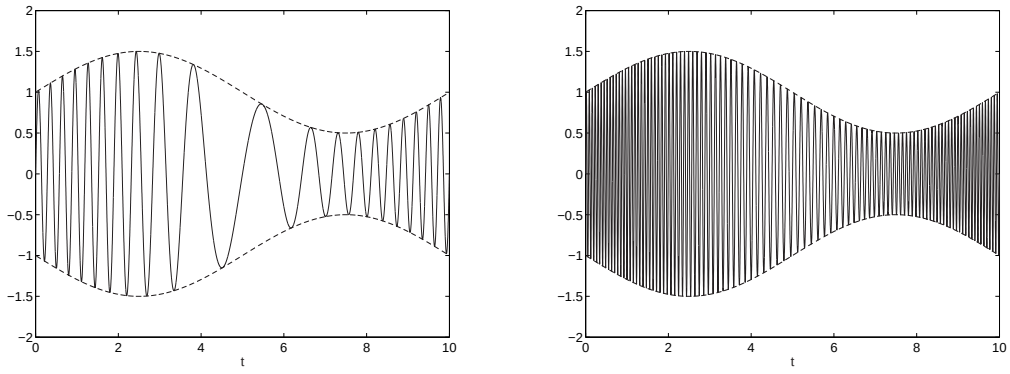

Figure 1: Signal x for moderate time scales (left) and for widely separated time scales (right).

properties. Furthermore, existing strategies for the determination of the local frequency function are outlined. Subsequently, we arrange the deciding functional and perform the according variational technique in Sect. 4. Finally, numerical results using a voltage controlled oscillator are demonstrated, where the presented strategy is employed.

2 Multivariate Signal Model

To outline the multidimensional model, we consider the RF signal

$$x(t) := \left[1 + \alpha \sin\left(\tfrac{2\pi}{T_1} t\right)\right] \cdot \sin\left(\tfrac{2\pi}{T_2} t + \beta \sin\left(\tfrac{2\pi}{T_1} t\right)\right) \tag{1}$$

with $T_1 > T_2$. Thereby, the parameters α and β introduce amplitude modulation (AM) and frequency modulation (FM), respectively. For $T_1 \gg T_2$, widely separated time scales arise, see Fig. 1. Thus we have to perform many time steps in order to resolve such a signal.

In the multivariate model, we assign an own variable to each separate time scale, which yields the function

$$\hat{x}(t_1, t_2) := \left[1 + \alpha \sin\left(\tfrac{2\pi}{T_1} t_1\right)\right] \cdot \sin\left(2\pi t_2 + \beta \sin\left(\tfrac{2\pi}{T_1} t_1\right)\right). \tag{2}$$

This new representation is called the *multivariate function* (*MVF*) of the signal. The MVF is biperiodic and thus already determined by its values in the rectangle $[0, T_1] \times [0, 1]$, where the second period is transformed from T_2 to 1. We reconstruct the original signal completely by its MVF via $x(t) = \hat{x}(t, t/T_2)$. Unfortunately, the MVF (2) exhibits many oscillations, see Fig. 2 (left). The

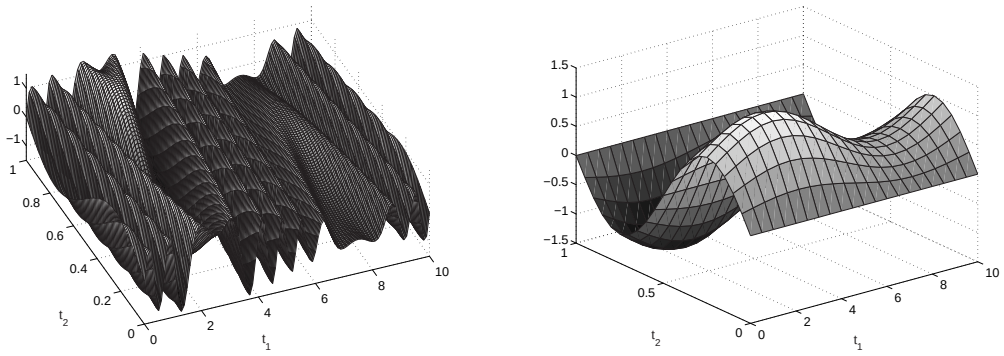

Figure 2: Inappropriate MVF $\hat{x}$ (left) vs. efficient MVF $\hat{y}$ (right).

number of oscillations increases with the amount of FM, i.e. the parameter β. Thus the representation (2) is inefficient.

Alternatively, we model AM and FM separately. The AM part is included in the new MVF

$$\hat{y}(t_1, t_2) := \left[1 + \alpha \sin\left(\tfrac{2\pi}{T_1} t_1\right)\right] \cdot \sin\left(2\pi t_2\right), \tag{3}$$

which owns a simple structure now, see Fig. 2 (right). Hence we can sample this MVF using relatively few grid points. On the other hand, the FM part is described by the time-dependent *warping function*

$$\Psi(t) := \frac{t}{T_2} + \frac{\beta}{2\pi} \sin\left(\tfrac{2\pi}{T_1} t\right). \tag{4}$$

Now the reconstruction of the original signal reads $x(t) = \hat{y}(t, \Psi(t))$, where the warping function stretches the second time scale. The derivative of the warping function can be interpreted as a local frequency of the signal, i.e.

$$\nu(t) := \Psi'(t) = \frac{1}{T_2} + \frac{\beta}{T_1} \cos\left(\tfrac{2\pi}{T_1} t\right). \tag{5}$$

Thus the local frequency represents an elementary T_1-periodic function. Consequently, we obtain an efficient model of the RF signal (1) by the MVF (3) and the local frequency (5).

The local frequency corresponding to the improper MVF (2) can be seen as $\nu \equiv 1/T_2$. Hence the selection of an appropriate local frequency function is crucial for the efficiency of the multivariate signal model.

3 Warped Multirate PDAE

Numerical simulation of electric circuits analyses the behaviour of all node voltages and some branch currents during a given time interval. Kirchhoff's laws generate systems of *differential algebraic equations* (*DAEs*) in the form

$$\frac{\mathrm{d}\mathbf{q}(\mathbf{x})}{\mathrm{d}t} = \mathbf{f}(\mathbf{x}(t)) + \mathbf{b}(t). \tag{6}$$

The arising functions in this DAE model represent the following quantities:

$\mathbf{x} : \mathbb{R} \to \mathbb{R}^k$	unknown voltages/currents,
$\mathbf{b} : \mathbb{R} \to \mathbb{R}^k$	independent input signals (voltages/currents),
$\mathbf{q} : \mathbb{R}^k \to \mathbb{R}^k$	terminal charges/branch fluxes,
$\mathbf{f} : \mathbb{R}^k \to \mathbb{R}^k$	currents of static elements/
	voltage drops of voltage controlling elements.

Since smooth solutions have to be determined, let $\mathbf{x}, \mathbf{q} \in C^1$ and $\mathbf{b}, \mathbf{f} \in C^0$. In the following, we assume that the input $\mathbf{b}$ is periodic with a slow rate T_1. Moreover, the solution $\mathbf{x}$ shall include a second time scale, which exhibits high frequency oscillations. Therefore the input generates AM and/or FM in the arising solution. In case of widely separated time scales, a transient analysis of the DAE model (6) demands an enormous amount of computational work, since the fast rate restricts the step sizes in time, while the slow rate specifies the time interval of the simulation.

Consequently, we change to the multivariate signal model described in the previous section. The transition to functions in several variables transforms the DAEs (6) into a system of *partial differential algebraic equations* (*PDAEs*). Brachtendorf et al. [1] introduced the according *multirate PDAE* for determining purely AM signals. Narayan and Roychowdhury [6] generalised the model for the additional presence of FM, which yields the *warped multirate PDAE*

$$\frac{\partial \mathbf{q}(\hat{\mathbf{x}})}{\partial t_1} + \nu(t_1)\frac{\partial \mathbf{q}(\hat{\mathbf{x}})}{\partial t_2} = \mathbf{f}(\hat{\mathbf{x}}(t_1, t_2)) + \mathbf{b}(t_1). \tag{7}$$

Thereby, $\hat{\mathbf{x}} : \mathbb{R}^2 \to \mathbb{R}^k$ represents the MVF of $\mathbf{x}$. Moreover, an a priori unknown local frequency function $\nu : \mathbb{R} \to \mathbb{R}$ arises, which describes the FM. Hence the system (7) is underdetermined and we require an additional condition to extract specific solutions. According to the other functions, let $\hat{\mathbf{x}} \in C^1$ and $\nu \in C^0$.

An arbitrary solution of the PDAE (7) yields a signal satisfying the DAE (6) via the reconstruction

$$\mathbf{x}(t) := \hat{\mathbf{x}}(t, \Psi(t)) \quad \text{with} \quad \Psi(t) := \textstyle\int_0^t \nu(\tau)\,\mathrm{d}\tau. \tag{8}$$

In this context, multiperiodic PDAE solutions produce RF signals of the desired type. More details about this connection in case of constant time rates can be found in [9]. Thus we compute $(T_1, 1)$-periodic MVFs $\hat{\mathbf{x}}$, where the second period is fixed to 1, corresponding to T_1-periodic local frequency functions ν. Although the presence of exactly two separate time scales is most frequently in RF signals, the multidimensional model can be generalised directly to the case of several time rates.

Now we analyse some properties of the PDAE (7). The system is autonomous in the second time scale. Therefore, given a solution $\hat{\mathbf{x}}$, the shifted function

$$\hat{\mathbf{y}}(t_1, t_2) := \hat{\mathbf{x}}\,(t_1, t_2 + c) \quad \text{with constant } \; c \in \mathbb{R} \tag{9}$$

also satisfies the PDAE including the same local frequency ν. Furthermore, the periodicities of the solution are preserved by the shifting. Hence this translation represents an inherent degree of freedom in the PDAE solution and thus in the reconstructed DAE solution, too. Hence we require an additional condition to isolate a solution from the continuum of shifted functions. This can be done by scalar phase conditions like

$$\hat{x}_1(0,0) = \eta \quad (\eta \in \mathbb{R}) \qquad \text{or} \qquad \frac{\partial \hat{x}_1}{\partial t_2}(0,0) = 0 \tag{10}$$

in the first component of the MVF $\hat{\mathbf{x}} = (\hat{x}_1, \ldots, \hat{x}_k)^\top$ without loss of generality.

Given a PDAE solution including a MVF and local frequency function, we obtain other solutions corresponding to different local frequencies via a transformation. The following assumptions shall be fulfilled:

$$\begin{aligned}
&\text{(i)} \quad \hat{\mathbf{x}} \in C^1(\mathbb{R}^2, \mathbb{R}^k) \quad \text{is } (T_1, 1)\text{-periodic,} \\
&\text{(ii)} \quad \nu \in C^0(\mathbb{R}, \mathbb{R}) \quad \text{is } T_1\text{-periodic,} \\
&\text{(iii)} \quad \mu \in C^0(\mathbb{R}, \mathbb{R}) \quad \text{is } T_1\text{-periodic,} \\
&\text{(iv)} \quad \textstyle\int_0^{T_1} \mu(\tau)\,\mathrm{d}\tau = \int_0^{T_1} \nu(\tau)\,\mathrm{d}\tau.
\end{aligned} \tag{11}$$

If $\hat{\mathbf{x}}$ and ν represent a solution of the PDAE system (7), then the transformed function $\hat{\mathbf{y}} \in C^1(\mathbb{R}^2, \mathbb{R}^k)$ with

$$\hat{\mathbf{y}}(t_1, t_2) := \hat{\mathbf{x}}\left(t_1, t_2 + \textstyle\int_0^{t_1} \nu(\tau) - \mu(\tau)\,\mathrm{d}\tau\right) \tag{12}$$

satisfies the PDAE including the local frequency function μ. Moreover, the new MVF $\hat{\mathbf{y}}$ is $(T_1, 1)$-periodic, too. If the assumptions (11) are not valid, then the transformation (12) also generates a PDAE solution. However, this solution is not biperiodic in general. In the following, we assume that the biperiodic boundary value problem of the PDAE system features a unique solution except for transformations of type (12) and translations of form (9).

It is easy to verify that PDAE solutions, which are interconnected by the transformation (12), reproduce the same DAE solution in the reconstruction (8), i.e.

$$\mathbf{x}(t) = \hat{\mathbf{x}}\left(t, \int_0^t \nu(\tau)\,\mathrm{d}\tau\right) = \hat{\mathbf{y}}\left(t, \int_0^t \mu(\tau)\,\mathrm{d}\tau\right). \tag{13}$$

Hence all solutions generated by the transformation (12) yield the desired information. Accordingly, we want to determine an uncomplex MVF in order to use relatively few grid points in a discretisation scheme. In addition, the local frequency function is physically reasonable, if and only if the corresponding MVF exhibits a simple structure, which is demonstrated by the example in Sect. 2.

The requirements (11) indicate the degree of freedom in the choice of the local frequency function. Given a solution $\hat{\mathbf{x}}$ and ν of the PDAE, where (i) and (ii) hold, we obtain another $(T_1, 1)$-periodic solution

$$\hat{\mathbf{y}}(t_1, t_2) := \hat{\mathbf{x}}\left(t_1, t_2 + \Theta(t_1)\right) \quad \text{with} \quad \Theta(t_1) := \int_0^{t_1} \theta(\tau)\,\mathrm{d}\tau \tag{14}$$

for an arbitrary T_1-periodic function $\theta : \mathbb{R} \to \mathbb{R}$ with $\int_0^{T_1} \theta(\tau)\,\mathrm{d}\tau = 0$. The corresponding T_1-periodic local frequency is given by $\mu(t_1) = \nu(t_1) - \theta(t_1)$. The defined function Θ satisfies the boundary conditions $\Theta(0) = \Theta(T_1) = 0$ and thus is T_1-periodic, too. Vice versa, the transformation (14) yields a biperiodic solution for an arbitrary T_1-periodic function $\Theta \in C^1$, which fulfils homogeneous boundary conditions.

Narayan and Roychowdhury [6] propose continuous phase conditions to determine the local frequency function and the corresponding MVF. The idea is to control the phase in each cross section of the MVF with constant t_1. Examples for continuous phase conditions are

$$\hat{x}_1(t_1, 0) = \eta \quad \text{for all } \; t_1 \in \mathbb{R}, \tag{15}$$

where a suitable constant $\eta \in \mathbb{R}$ is used, or

$$\frac{\partial \hat{x}_1}{\partial t_2}(t_1, 0) = 0 \quad \text{for all } \; t_1 \in \mathbb{R} \tag{16}$$

in the, without loss of generality, first component of the MVF. Hence we obtain additional boundary conditions in the domain of dependence. Thereby, a solution from the continuum given by (9) is specified automatically. Based on the transformation formula (12), the existence of corresponding PDAE solutions can be motivated using the implicit function theorem. The strategy applies for initial/boundary value problems as well as for biperiodic boundary value problems. Numerical simulations confirm that the phase conditions (15) and (16) yield simple MVFs, see [8]. The requirements imply that one component of the MVF exhibits an elementary form on the line $t_2 = 0$. However, we can not guarantee that the complete MVF exhibits an adequate structure in general.

Alternatively, Houben [4] introduces a minimisation technique, which shall generate MVFs with a relatively low amount of change with respect to the first coordinate direction. In this approach, the magnitude

$$s(t_1) := \int_0^1 \left\| \frac{\partial \mathbf{q}(\hat{\mathbf{x}})}{\partial t_1} \right\|^2 \, \mathrm{d}t_2 \tag{17}$$

is minimised for each $t_1 > 0$, where the Euclidean norm $\|\cdot\|$ in $\mathbb{R}^k$ is applied. The important quality is that the partial derivative in (17) can be replaced by the other terms in the PDAE (7). Consequently, an according calculus yields an explicit formula for the resulting optimal local frequency function in dependence on the MVF. The strategy is constructed for solving a mixture of initial and boundary conditions. Starting from initial values in $t_1 = 0$, the PDAE is solved by progression in the first coordinate direction, while regarding the periodicity in the second coordinate direction. Test results show that this technique produces elementary MVFs, too, see [4]. However, the minimisation is based on $\mathbf{q}(\hat{\mathbf{x}})$ instead of the MVF $\hat{\mathbf{x}}$ itself in order to use information from the PDAE. Some components of the MVF may not influence the function $\mathbf{q}(\hat{\mathbf{x}})$ at all and thus can not be controlled. For example, if the underlying DAE (6) is semi-explicit, then algebraic variables do not appear in $\mathbf{q}(\hat{\mathbf{x}})$. Furthermore, we can not perform an adequate weighting in each component of the MVF here, which is necessary in case of largely differing physical units in the system.

4 Variational Technique

We consider biperiodic boundary value problems of the PDAE in the following. As we have seen in Sect. 2, an inappropriate choice of the local frequency function results in an oscillatory MVF. Thereby, the number of oscillations within the domain $[0, T_1] \times [0, 1]$ can become arbitrarily large. According to (17), the idea is to decrease oscillating behaviour in the MVFs by minimising some amount of change. Now we apply the MVF directly in the minimisation. Consequently, the magnitude of arising partial derivatives has to be quantified.

Let $\hat{\mathbf{x}} = (\hat{x}_1, \ldots, \hat{x}_k)^\top$ be the components of a $(T_1, 1)$-periodic MVF. We define the functional $\gamma : C^1(\mathbb{R}^2, \mathbb{R}^k) \to \mathbb{R}_0^+$ via

$$\gamma\left(\hat{\mathbf{x}}\right) := T_1 \int_0^{T_1} \int_0^1 \sum_{l=1}^{k} w_l \left(\frac{\partial \hat{x}_l}{\partial t_1} \right)^2 \, \mathrm{d}t_2 \, \mathrm{d}t_1 \tag{18}$$

using constant weights $w_l \geq 0$ for $l = 1, \ldots, k$. This formula describes only the amount of change with respect to the first coordinate direction. The transformation (12) does not affect the total change in the second coordinate direction.

Hence, using the alternative functional $\tilde{\gamma} : C^1(\mathbb{R}^2, \mathbb{R}^k) \to \mathbb{R}_0^+$ with

$$\tilde{\gamma}\left(\hat{\mathbf{x}}\right) := \frac{1}{T_1} \int_0^{T_1} \int_0^1 \sum_{l=1}^{k} \tilde{w}_l \left(\frac{\partial \hat{x}_l}{\partial t_2}\right)^2 \, \mathrm{d}t_2 \, \mathrm{d}t_1, \tag{19}$$

it holds $\tilde{\gamma}(\hat{\mathbf{x}}) = \tilde{\gamma}(\hat{\mathbf{y}})$ whenever $\hat{\mathbf{x}}, \hat{\mathbf{y}}$ are related via (12) under the assumptions (11). The proof is straightforward. Therefore, instead of combining (18) and (19), we just employ the first functional. Furthermore, we recognise that both functionals are invariant with respect to translations of type (9) in case of biperiodic MVFs. Remark also that setting some weights equal to zero enables to focus on an arbitrary subset of components, which allows some flexibility.

To perform the following calculus, we assume $\hat{\mathbf{x}} \in C^2(\mathbb{R}^2, \mathbb{R}^k)$ for all arising MVFs. Let $\hat{\mathbf{x}}_{\mathrm{opt}}$ be an optimal solution, i.e. a global minimum of the functional (18), corresponding to a local frequency ν_{opt}. Applying transformations of type (14), we obtain competitive MVFs

$$\hat{\mathbf{y}}_\varepsilon(t_1, t_2) := \hat{\mathbf{x}}_{\mathrm{opt}}\left(t_1, t_2 + \varepsilon\Theta(t_1)\right) \quad \text{for each } \varepsilon \in \mathbb{R} \tag{20}$$

including an arbitrary T_1-periodic $\Theta \in C^1(\mathbb{R}, \mathbb{R})$ satisfying $\Theta(0) = \Theta(T_1) = 0$. The optimal behaviour of the MVF implies

$$\gamma(\hat{\mathbf{y}}_\varepsilon) \geq \gamma(\hat{\mathbf{x}}_{\mathrm{opt}}) \quad \text{for all } \varepsilon \in \mathbb{R}. \tag{21}$$

To simplify notation, we suppress the location $(t_1, t_2 + \varepsilon\Theta(t_1))$ of function evaluations in the following. Let $\hat{\mathbf{x}}_{\mathrm{opt}} = (\hat{x}_1, \ldots, \hat{x}_k)^\top$ be the components of an optimal function now. It follows that the functional (18) corresponding to a competitive MVF (20) exhibits the formula

$$\gamma(\hat{\mathbf{y}}_\varepsilon) = T_1 \int_0^{T_1} \int_0^1 \sum_{l=1}^{k} w_l \left(\frac{\partial \hat{x}_l}{\partial t_1} + \varepsilon\Theta' \frac{\partial \hat{x}_l}{\partial t_2}\right)^2 \, \mathrm{d}t_2 \, \mathrm{d}t_1. \tag{22}$$

We differentiate the functional with respect to ε and thus obtain

$$\begin{aligned} \frac{\mathrm{d}\gamma(\hat{\mathbf{y}}_\varepsilon)}{\mathrm{d}\varepsilon} \;=\; & 2T_1 \int_0^{T_1} \int_0^1 \sum_{l=1}^{k} w_l \left(\frac{\partial \hat{x}_l}{\partial t_1} + \varepsilon\Theta' \frac{\partial \hat{x}_l}{\partial t_2}\right) \\ & \cdot \left(\Theta \frac{\partial^2 \hat{x}_l}{\partial t_1 \partial t_2} + \varepsilon\Theta\Theta' \frac{\partial^2 \hat{x}_l}{\partial {t_2}^2} + \Theta' \frac{\partial \hat{x}_l}{\partial t_2}\right) \, \mathrm{d}t_2 \, \mathrm{d}t_1. \end{aligned} \tag{23}$$

A necessary condition for a global minimum with respect to the underlying functional (18) is given by

$$\left.\frac{\mathrm{d}\gamma(\hat{\mathbf{y}}_\varepsilon)}{\mathrm{d}\varepsilon}\right|_{\varepsilon=0} = 0. \tag{24}$$

Setting $\varepsilon = 0$ recovers the location (t_1, t_2) for function evaluations. We omit this notation in the following, too. Consequently, (23) and (24) imply

$$\int_0^{T_1} \int_0^1 \sum_{l=1}^{k} w_l \cdot \frac{\partial \hat{x}_l}{\partial t_1} \cdot \left(\Theta \frac{\partial^2 \hat{x}_l}{\partial t_1 \partial t_2} + \Theta' \frac{\partial \hat{x}_l}{\partial t_2} \right) \, \mathrm{d}t_2 \, \mathrm{d}t_1 = 0. \tag{25}$$

Integration by parts with regard to $\Theta(0) = \Theta(T_1) = 0$ yields

$$\int_0^{T_1} \left(\frac{\partial \hat{x}_l}{\partial t_1} \cdot \frac{\partial \hat{x}_l}{\partial t_2} \right) \cdot \Theta' \, \mathrm{d}t_1 = - \int_0^{T_1} \left(\frac{\partial^2 \hat{x}_l}{\partial {t_1}^2} \cdot \frac{\partial \hat{x}_l}{\partial t_2} + \frac{\partial \hat{x}_l}{\partial t_1} \cdot \frac{\partial^2 \hat{x}_l}{\partial t_1 \partial t_2} \right) \cdot \Theta \, \mathrm{d}t_1. \tag{26}$$

Thus one term in (25) drops out and we get

$$\int_0^{T_1} \left[\int_0^1 \sum_{l=1}^{k} w_l \cdot \frac{\partial^2 \hat{x}_l}{\partial {t_1}^2} \cdot \frac{\partial \hat{x}_l}{\partial t_2} \, \mathrm{d}t_2 \right] \cdot \Theta \, \mathrm{d}t_1 = 0. \tag{27}$$

This relation holds for all T_1-periodic functions $\Theta \in C^1$ with $\Theta(0) = \Theta(T_1) = 0$. The fundamental lemma of variational calculus assumes arbitrary smooth functions fulfilling homogeneous boundary conditions. Nevertheless, the result remains the same under the restriction to periodic functions. Consequently, property (27) implies

$$r(t_1) := \int_0^1 \sum_{l=1}^{k} w_l \cdot \frac{\partial^2 \hat{x}_l}{\partial {t_1}^2} \cdot \frac{\partial \hat{x}_l}{\partial t_2} \, \mathrm{d}t_2 = 0 \quad \text{for all } \; t_1 \in \mathbb{R}. \tag{28}$$

Hence we obtain a necessary condition, which the MVF has to satisfy in order to be an optimal solution. We see that the resulting structure agrees with the free parameters, i.e. the local frequency, in the PDAE system. The local frequency ν represents a scalar function depending on t_1. Likewise, the scalar function r in (28) depends on t_1 and describes the additional condition to determine the local frequency.

It is interesting to see the result of the variational calculus applied to the unhelpful functional (19). In this case, the necessary condition reads

$$\tilde{r}(t_1) := \int_0^1 \sum_{l=1}^{k} \tilde{w}_l \cdot \frac{\partial^2 \hat{x}_l}{\partial {t_2}^2} \cdot \frac{\partial \hat{x}_l}{\partial t_2} \, \mathrm{d}t_2 = 0 \quad \text{for all } \; t_1 \in \mathbb{R}. \tag{29}$$

Considering the periodicity of $\hat{\mathbf{x}}$ in the variable t_2, integration by parts proves

$$\int_0^1 \frac{\partial^2 \hat{x}_l}{\partial {t_2}^2} \cdot \frac{\partial \hat{x}_l}{\partial t_2} \, \mathrm{d}t_2 = 0 \quad \text{for } \; l = 1, \ldots, k. \tag{30}$$

Consequently, condition (29) is always satisfied. This property reflects the fact that the functional (19) is invariant with respect to transformations (12).

Now we can apply the condition (28) in a numerical method to compute the MVF $\hat{\mathbf{x}}$ as well as the local frequency ν. Newton's method yields an approximative solution of arising nonlinear systems. Thereby, the choice of starting values is critical for the convergence of the iteration. We suggest the following strategy. Replacing the input signals $\mathbf{b}$ in (6) by constant mean values $\mathbf{b}_0$ results in the autonomous DAE

$$\frac{\mathrm{d}\mathbf{q}(\mathbf{x})}{\mathrm{d}t} = \mathbf{f}(\mathbf{x}(t)) + \mathbf{b}_0. \tag{31}$$

If a corresponding periodic solution $\mathbf{x}_{\mathrm{per}} : \mathbb{R} \to \mathbb{R}$ exists, then we compute this function and its period T_0 by methods described in [5], for example. We define

$$\hat{\mathbf{x}}(t_1, t_2) := \mathbf{x}_{\mathrm{per}}(t_2), \qquad \nu(t_1) :\equiv 1/T_0 \tag{32}$$

and use these functions as starting values in a Newton iteration. It holds $\gamma(\hat{\mathbf{x}}) = 0$, i.e. this choice represents a global minimum of the functional (18). Thus we may expect that (32) yields good starting values for the optimal PDAE solution.

However, the outlined strategy is often not sufficient for convergence. In this case, we apply a homotopy method based on the PDAE

$$\frac{\partial \mathbf{q}(\hat{\mathbf{x}})}{\partial t_1} + \nu(t_1)\frac{\partial \mathbf{q}(\hat{\mathbf{x}})}{\partial t_2} = \mathbf{f}(\hat{\mathbf{x}}(t_1, t_2)) + \lambda\left(\mathbf{b}(t_1) - \mathbf{b}_0\right) + \mathbf{b}_0 \tag{33}$$

with parameter $\lambda \in [0, 1]$. For $\lambda = 0$, a PDAE arises, where a solution is given by (32). For $\lambda = 1$, we obtain the desired system. Accordingly, small step sizes with respect to the parameter λ assure that the solution of one step represents good starting values for the subsequent step. A physical interpretation of this homotopy method means to supply the electric circuit with appropriate input signals. The technique can be used in any numerical scheme solving the PDAE system.

The computational effort in numerical methods, which apply the additional condition from the variational technique, is not significantly higher in comparison to methods using continuous phase conditions like (15) or (16), although evaluations of (28) demand more costs and involve more unknowns. The solution of the PDAE system causes the main part of computational work, since corresponding discretisations exhibit a two-dimensional structure, whereas the additional constraints represent one-dimensional requirements.

Finally, we remark that other choices of the functional to be minimised are feasible, where variational calculus can be applied in the same way. For example, according to (17), derivatives of the MVF $\hat{\mathbf{x}}$ can be substituted by derivatives of $\mathbf{q}(\hat{\mathbf{x}})$. Furthermore, instead of integrating the whole domain of dependence, the minimisation can be restricted to initial values of the MVF on the line $t_2 = 0$.

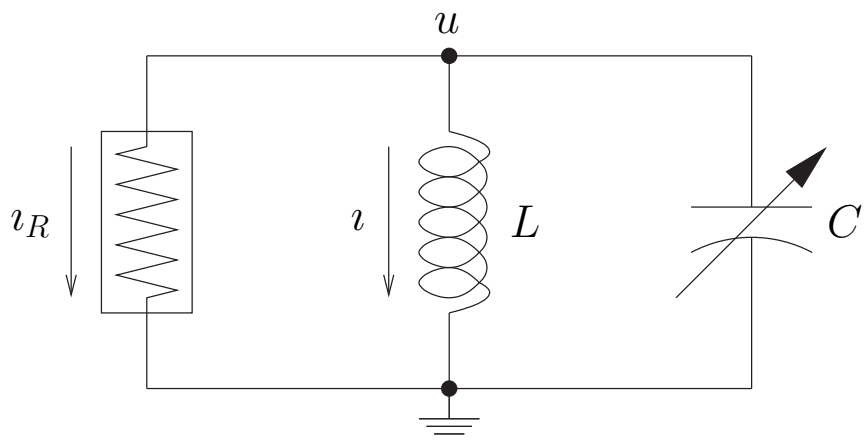

Figure 3: Circuit diagram of voltage controlled oscillator.

5 Illustrative Example

To apply the constructed technique, we consider a DAE system modelling a *voltage controlled oscillator*. Fig. 5 illustrates the corresponding circuit diagram, where a capacitance, an inductance and a nonlinear resistor arise. Thereby, the capacitance is controlled by an additional input signal and thus becomes time-dependent. This circuit is designed similarly to the test example in [6]. A mathematical description yields system

$$\begin{aligned} \dot{u} &= \left(-\imath_R(u) - \imath\right)/(Cz) \\ \dot{\imath} &= u/L \\ 0 &= z - b(t), \end{aligned} \tag{34}$$

which represents a semi-explicit DAE of index 1. More details concerning the index concept with respect to electric circuits can be found in [3]. The unknown functions are the node voltage u [V], the branch current $\imath$ [A] and the variable z, which reproduces the input signal. The input signal b owns no physical unit, because it describes a relative change of the capacitance in the system (34). We select the harmonic oscillation

$$b(t) = 1 + 0.8\cos\left(\tfrac{2\pi}{T_1}t\right) \tag{35}$$

using the slow rate $T_1 = 1$ ms, which accords to a frequency of 1 kHz. The current-voltage relation of the nonlinear resistor is given by the function

$$\imath_R(u) = (G_0 - G_\infty)U_k \tanh\left(\frac{u}{U_k}\right) + G_\infty u. \tag{36}$$

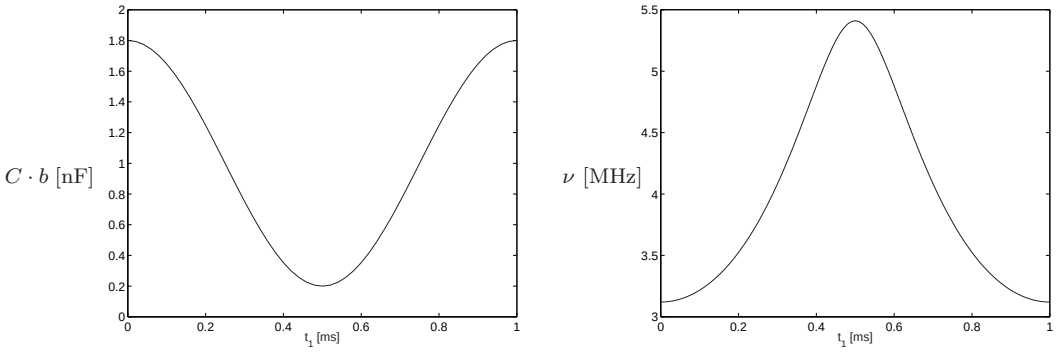

Figure 4: Capacitance (left) and optimal local frequency (right).

In our simulations, the used technical parameters are

$$C = 1 \text{ nF}, \quad L = 1\ \mu\text{H}, \quad U_k = 1 \text{ V}, \quad G_0 = -0.1 \text{ A/V}, \quad G_\infty = 0.25 \text{ A/V}.$$

For constant input $b \equiv 1$, the DAE system exhibits a periodic oscillation with a high frequency about 4 MHz. The time-dependent input (35) generates AM and FM at largely differing time scales. Consequently, we change to the PDAE model (7), where we apply the additional condition (28) from the variational technique. The weights are set to $w_l = 1$ for all l. Furthermore, we use the first scalar phase condition in (10) with $\eta = 0$ to fix a solution. In the PDAE system, partial derivatives are discretised on a uniform grid employing asymmetric formulae of second order. Likewise, we evaluate the requirement (28) by approximations based on values in the grid points. The arising nonlinear system is solved by Newton iterations, where we utilise the homotopy method explained in the previous section. The input signal and the resulting local frequency function are given in Fig. 4. As expected for LC-oscillators, low capacitances cause high frequencies in a nonlinear correlation. Hence the computed local frequency is physically reasonable. The simple form of the corresponding MVFs, which are illustrated in Fig. 5, confirms this fact.

To justify the optimal behaviour of the obtained solution, we apply transformation (12) to calculate some competitive solutions. Thereby, the new local frequency functions read

$$\mu(t_1) := \nu_{\text{opt}}(t_1) + \alpha_0 \left(\tfrac{1}{T_1} \int_0^{T_1} \nu_{\text{opt}}(\tau)\, \mathrm{d}\tau \right) \sin\left(\tfrac{2\pi}{T_1} t_1 \right), \tag{37}$$

where a parameter $\alpha_0 \in \mathbb{R}$ is used. Since an integral mean value is included, the parameter α_0 represents a relative magnitude of the perturbation in comparison to the optimal local frequency. The new local frequency satisfies our assumptions (iii) and (iv) in (11) required for the transformation. Now we employ formula (12) to compute the corresponding MVFs. The following table illustrates the resulting values of the functional (18) evaluated for these competitive MVFs.

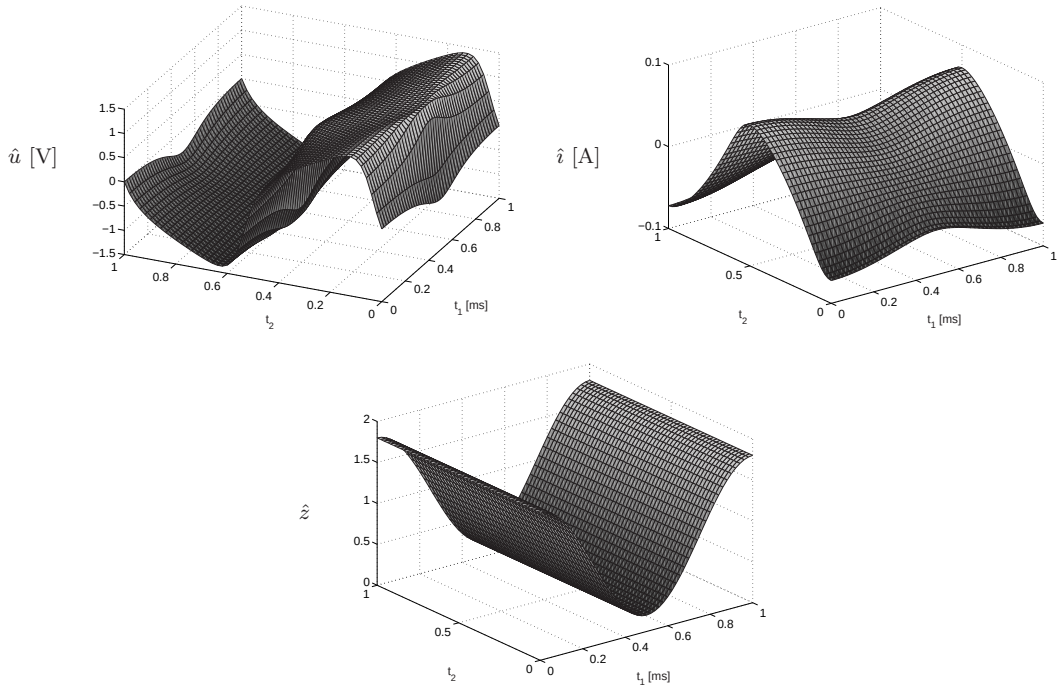

Figure 5: Optimal MVFs for each component.

α_0	10^{-3}	10^{-4}	10^{-5}	0	-10^{-5}	-10^{-4}	-10^{-3}
$\gamma(\hat{\mathbf{x}}_\mu)$	515.53	18.82	12.94	12.89	12.94	18.81	509.96

We recognise that the minimum is reached for $\alpha_0 = 0$, which recovers the local frequency ν_{opt} computed by the variational technique. Moreover, the magnitude of the functional increases rapidly the more the parameter α_0 differs from zero.

Furthermore, we compute a PDAE solution using the continuous phase condition (15) with $\eta = 0$. Fig. 6 demonstrates the resulting local frequency and the MVF of u. Differences to the optimal local frequency are tiny, namely less than a relative magnitude of 10^{-4}. In contrast, a small discrepancy is visible in the MVFs. Thus moderate changes of the local frequency function cause huge deformations in the corresponding MVFs in case of widely separated time scales, see [7] for further details. Despite this sensitivity, the presented methods produce correct solutions, since the local frequency is not prescribed but determined indirectly by the corresponding MVF. The value of the functional (18) results to $\gamma = 13.06$ in the latter simulation, which is very close to the optimal value. Hence continuous phase conditions permit efficient simulations of the PDAE model, too. However, this behaviour is heuristic and an according strict justification is missing.

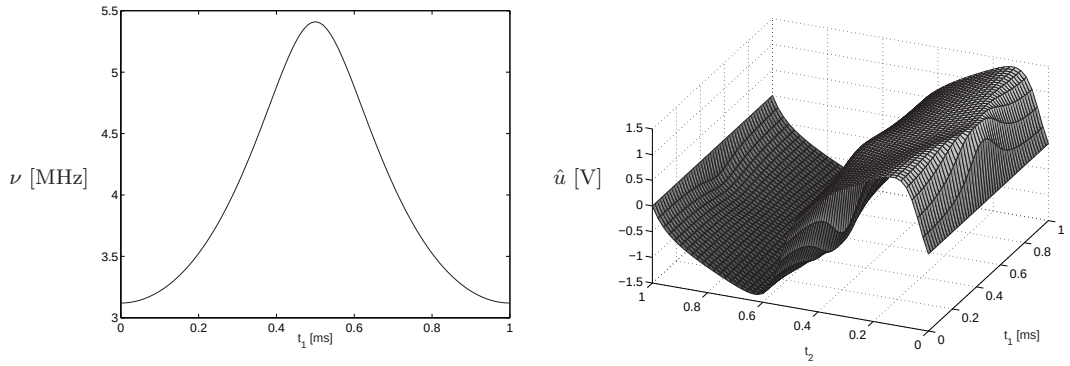

Figure 6: Local frequency ν (left) and MVF $\hat{u}$ (right) corresponding to simulation using continuous phase condition.

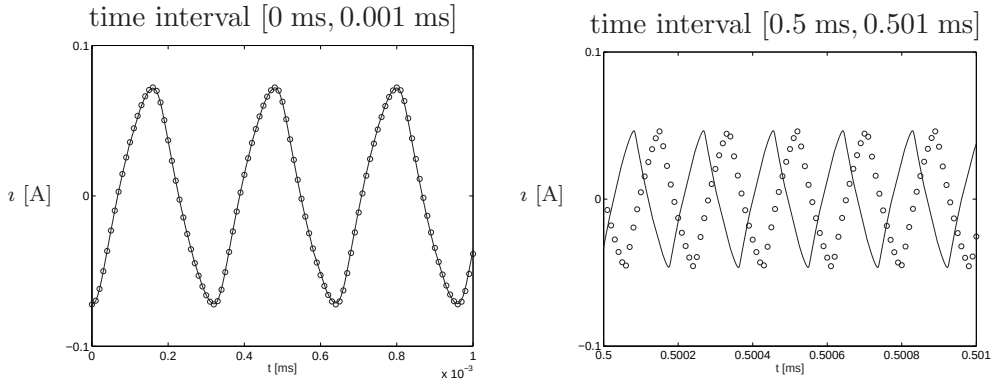

Figure 7: DAE solution for $\imath$ reconstructed by PDAE solution (circles) and computed by transient analysis (solid line).

Finally, we use the computed optimal PDAE solution to obtain corresponding RF signals satisfying the DAE via the reconstruction (8). For comparison, a transient analysis of the DAE system is performed applying trapezoidal rule, where values of the PDAE solution provide the initial condition. Fig. 7 displays the outcome for the current $\imath$ in different time intervals. In the first few cycles, the two signals exhibit an excellent agreement. In later cycles, a phase shift emerges between both approximations, which is produced by two effects. Firstly, small numerical errors in the local frequency function amplify during many oscillations. Secondly, the trapezoidal rule causes a phase shift in comparison to the exact solution, too, which is typical for such integration schemes. Nevertheless, the other properties of the signal agree in later cycles, i.e. the amplitude, the frequency and the shape. We recognise AM and FM in this component. During the time interval $[0, T_1]$, about 4 000 oscillations arise, which can be reconstructed by the PDAE solution.

6 Conclusions

The multidimensional model based on warped multirate PDAEs provides an efficient simulation of RF signals, if an arising local frequency function is selected suitably. For this purpose, a minimum demand has been imposed on the corresponding multivariate solution in case of biperiodic boundary value problems. A transformation formula connecting feasible solutions has enabled a variational calculus, which produces a necessary condition for an optimal solution. The structure of the arising constraint agrees to the degree of freedom in the PDAE caused by the included local frequency function. According numerical simulations, where the additional condition from the variational technique is used, validate the efficiency of the presented approach. Furthermore, the designed strategy can be generalised to the minimisation of other functionals in this context.

Acknowledgements

This work has been supported within the federal BMBF project No. 03GUNAVN. The author is indebted to Prof. M. Günther (University of Wuppertal) and S. Knorr (University of Wuppertal) for helpful discussions. In addition, the author thanks T. Mei (University of Minnesota) for informations about the used example of the voltage controlled oscillator.

References

[1] Brachtendorf, H. G.; Welsch, G.; Laur, R.; Bunse-Gerstner, A.: Numerical steady state analysis of electronic circuits driven by multi-tone signals. Electrical Engineering 79 (1996), pp. 103-112.

[2] Günther, M.; Feldmann, U.: CAD based electric circuit modeling in industry I: mathematical structure and index of network equations. Surv. Math. Ind. 8 (1999), pp. 97-129.

[3] Günther, M.; Rentrop, P.: The differential-algebraic index concept in electric circuit simulation. Z. Angew. Math. Mech. 76 (1996) 1, pp. 91-94.

[4] Houben, S.H.M.J.: Simulating multi-tone free-running oscillators with optimal sweep following. In: Schilders, W.H.A., ter Maten, E.J.W., Houben, S.H.M.J. (eds.): Scientific Computing in Electrical Engineering, Mathematics in Industry, Springer, 2004, pp. 240-247.

[5] Kundert, K. S.; Sangiovanni-Vincentelli, A.; Sugawara, T.: Techniques for finding the periodic steady-state response of circuits. In: Ozawa, T. (Ed.): Analog methods for computer-aided circuit analysis and diagnosis. New York 1988, pp. 169-203.

[6] Narayan, O.; Roychowdhury, J.: Analyzing oscillators using multitime PDEs. IEEE Trans. CAS I 50 (2003) 7, pp. 894-903.

[7] Pulch, R.: Multi time scale differential equations for simulating frequency modulated signals. Appl. Numer. Math. 53 (2005) 2-4, pp. 421-436.

[8] Pulch, R.: Warped MPDAE models with continuous phase conditions. to appear in: Proceeding of ECMI conference, Eindhoven 2004.

[9] Roychowdhury, J.: Analysing circuits with widely-separated time scales using numerical PDE methods. IEEE Trans. CAS I 48 (2001) 5, pp. 578-594.